Efficient Channel Estimation in Millimeter Wave Hybrid MIMO Systems with Low Resolution ADCs

Aryan Kaushik, Evangelos Vlachos, John Thompson, and Alessandro Perelli
Institute for Digital Communications, The University of Edinburgh, United Kingdom.
Email: {A.Kaushik, E.Vlachos, J.S.Thompson, A. Perelli}@ed.ac.uk

***Abstract*—This paper proposes an efficient channel estimation algorithm for millimeter wave (mmWave) systems with a hybrid analog-digital multiple-input multiple-output (MIMO) architecture and few-bits quantization at the receiver. The sparsity of the mmWave MIMO channel is exploited for the problem formulation while limited resolution analog-to-digital converters (ADCs) are used in the receiver architecture. The estimation problem can be tackled using compressed sensing through the Stein's unbiased risk estimate (SURE) based parametric denoiser with the generalized approximate message passing (GAMP) framework. Expectation-maximization (EM) density estimation is used to avoid the need of specifying channel statistics resulting the EM-SURE-GAMP algorithm to estimate the channel. SURE, depending on the noisy observation, is minimized to adaptively optimize the denoiser within the parametric class at each iteration. The proposed solution is compared with the expectation-maximization generalized AMP (EM-GAMP) solution and the mean square error (MSE) performs better with respect to low and high signal-to-noise ratio (SNR) regimes, the number of ADC bits, and the training length. The use of the low resolution ADCs reduces power consumption and leads to an efficient mmWave MIMO system.**

***Keywords*—channel estimation, low resolution analog-to-digital converter (ADC), compressed sensing, mmWave MIMO.**

I. Introduction

The large number of antenna elements associated with millimeter wave (mmWave) multiple input multiple output (MIMO) systems makes it hard to use many analog-to-digital converters (ADCs), which is a power hungry component [1]. Moreover, ADCs have much higher sampling rates for wide bandwidth mmWave systems than at microwave frequencies, and employing high speed ADCs increases the power consumption and the cost significantly [2], [3]. Implementing low resolution ADCs such as 1-bit to 3-bits in mmWave MIMO systems efficiently improves the power metric of the system [1]. Fig. 1 shows the hardware block diagram of a mmWave system with a hybrid analog-digital architecture and low resolution ADCs at the receiver. The use of 1-bit ADCs in MIMO systems has been discussed in [4] and [5], and channel estimation is investigated as well. In that work, the channel is known perfectly to the transmitter and the receiver while in practical scenarios, the channel state information (CSI) is not known and should be estimated by both the transmitter and the receiver.

References [6]-[8] estimate the sparse mmWave channel using signal processing tools for high resolution analog to digital converting structures, but the use of low resolution ADCs at the receiver can significantly reduce the power consumption without significantly affecting the capacity of the system [9]. Recently, [10] and [11] considered 1-bit ADC quantization systems and the sparsity in the angle domain is exploited to be able to use compressed sensing (CS) techniques to recover the channel parameters. The proposed adaptive technique in [10] fails to provide good estimation of the channel at low SNR values. Reference [11] proposes only an expectation-maximization (EM) algorithm which has high complexity since each iteration requires a matrix inverse computation and convergence of the algorithm requires many iterations. To observe the effect of low resolution ADCs, an additive quantization model (AQNM) is considered in [12] and [13]. The effect of AQNM is investigated in [12] for the case of a point-to-point mmWave MIMO system, while in [13] the desired rate of the uplink was derived for the case of mmWave fading channels. References [14] and [15] also implement the EM algorithm for a MIMO channel. Further improvements to the EM algorithm are proposed using expectation-maximization generalized approximate message passing (EM-GAMP) [16] and vector approximate message passing (VAMP) [17]. The use of EM-GAMP has been exploited for a broadband mmWave MIMO channel model with low resolution ADCs at the receiver in [18].

Reference [19] describes the advantages of the Stein's unbiased risk estimate (SURE) based parametric denoiser when incorporated with the approximate message passing (AMP) framework. This paper exploits the SURE-generalized AMP solution combined with expectation-maximization (EM) steps called the EM-SURE-GAMP in a mmWave MIMO system. This novel solution avoids strong assumptions on the channel statistics where SURE, depending on the noisy observation, is minimized to adaptively optimize the denoiser within the parametric class at each iteration. The proposed solution is compared with the EM-GAMP solution for a narrowband channel model and improved mean square error (MSE) performance is observed for both low and high signal-to-noise ratio (SNR) regimes. The unknown channel parameters are modeled by a Bernoulli Gaussian distribution for both the techniques.

Notations: x, $\mathbf{x}$, and $\mathbf{X}$, represent a scalar, a vector, and a matrix, respectively; the i^{th} column of $\mathbf{X}$ is $\mathbf{X}^{(i)}$; the transpose of $\mathbf{X}$ is $\mathbf{X}^T$ while the conjugate transpose is $\mathbf{X}^*$; tr($\mathbf{X}$) and $|\mathbf{X}|$, are the trace and determinant of $\mathbf{X}$, while $||\mathbf{X}||_F$ is the Frobenius norm; the p-norm of $\mathbf{x}$ is $||\mathbf{x}||_p$; $\mathbf{X} \otimes \mathbf{Y}$ represents the Kronecker product of $\mathbf{X}$ and $\mathbf{Y}$, diag($\mathbf{X}$) generates a vector of the diagonal elements of $\mathbf{X}$; vec($\mathbf{X}$) is a vector showing all the columns of $\mathbf{X}$, $\mathbf{I}_N$ represents an identity matrix of dimension $N \times N$ and $\mathbf{0}_{A\times B}$ is an all-zeros matrix of dimension $A \times B$. $\mathbb{E}[.]$ represents the expectation of a complex variable. $\mathbb{R}^{A\times B}$ and $\mathbb{C}^{A\times B}$ denote the set of

ISBN 978-90-827970-1-5 © EURASIP 2018

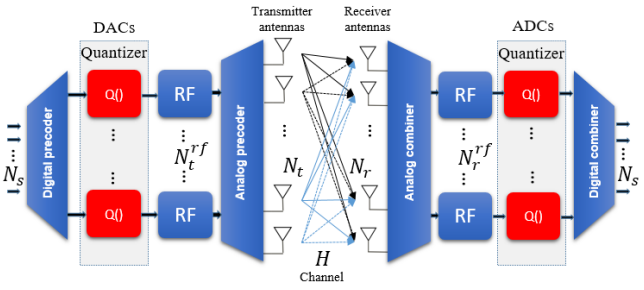

Fig. 1: MmWave system with a hybrid analog-digital MIMO architecture and low resolution ADCs at the receiver.

$A \times B$ matrices with real and complex entries, respectively. A complex Gaussian vector with mean $\mathbf{x}$ and covariance matrix as $\mathbf{X}$ is represented as $\mathcal{CN}(\mathbf{x}; \mathbf{X})$, and i.i.d. indicates the entries to be independent and identically distributed.

II. MmWave Hybrid MIMO Model

The high path loss and small number of multi-path components in mmWave MIMO systems restrict use of the fading channels used in the analysis of MIMO systems [1]. Consider a single-user mmWave MIMO system with N_t antennas at the transmitter, with N_s transmitted data streams to N_r receiver antennas. For the number of multipaths computed by the product of N_{cl} clusters and N_{ray} rays in every cluster, the narrowband channel is written as follows:

$$\mathbf{H} = \sum_{i=1}^{N_{cl}} \sum_{l=1}^{N_{ray}} \alpha_{il} \mathbf{a}_r(\phi_{il}^r) \mathbf{a}_t(\phi_{il}^t)^*, \quad (1)$$

α_{il} in (1) is the complex gain of l^{th} ray in i^{th} cluster; $\mathbf{a}_t(\phi_{il}^t)$ and $\mathbf{a}_r(\phi_{il}^r)$ are the normalized transmit and receive array response vectors, where ϕ_{il}^t and ϕ_{il}^r are the elevation angles of departure and arrival, respectively. We modeled the antenna elements as ideal sectored elements at both the transmitter and the receiver [20]. In (1), the transmit and receive antenna element gains are considered unity over the sectors defined by $\phi_{il}^t \in [\phi_{min}^t, \phi_{max}^t]$ and $\phi_{il}^r \in [\phi_{min}^r, \phi_{max}^r]$, respectively. We implement uniform linear array (ULA) geometry. For λ signal wavelength, d inter-element spacing, and a ULA geometry with N_z antenna elements, the array response vector is written as follows [21]:

$$\mathbf{a}_z(\phi) = \frac{1}{\sqrt{N_z}} [1, e^{j\frac{2\pi}{\lambda} d \sin(\phi)}, ..., e^{j(N_z-1)\frac{2\pi}{\lambda} d \sin(\phi)}]^T, \quad (2)$$

Equation (2) can be used to compute the array response vectors at both the transmitter and receiver with the corresponding terms. The beamspace representation [22], [23] of the narrowband channel in (1) can be written as follows:

$$\mathbf{H} = \hat{\mathbf{A}}_r \mathbf{Z} \hat{\mathbf{A}}_t^*, \quad (3)$$

where $\mathbf{Z} \in \mathbb{C}^{N_r \times N_t}$ represents a sparse matrix with a few non-zero entries assumed to follow Bernoulli-Gaussian distribution, while $\hat{\mathbf{A}}_r \in \mathbb{C}^{N_r \times N_r}$ and $\hat{\mathbf{A}}_t \in \mathbb{C}^{N_t \times N_t}$ are DFT matrices.

Let us consider a MIMO $N_t \times N_r$ system with a hybrid analog-digital architecture with N_t^{rf} and N_r^{rf} chains at the transmitter and the receiver, respectively. The number of RF chains is smaller or equal to the number of antennas for both the transmitter $N_t^{rf} \leq N_t$ and the receiver $N_r^{rf} \leq N_r$. We assume that the channel is quasi-static, i.e., it remains static during a period of time, which includes both channel training and data transmission phases. During the training phase, at each time instance t, the transmitter generates a training signal vector $\mathbf{s}(t) \in \mathbb{C}^{N_t^{rf} \times 1}$ following $\mathbb{E}[\mathbf{s}(t)\mathbf{s}(t)^*] = \frac{1}{N_s}\mathbf{I}_{N_s}$, which is the input to the analog RF precoder at transmitter, $\mathbf{F}_{rf}(t) \in \mathbb{C}^{N_t \times N_t^{rf}}$. This signal is transmitted through the channel $\mathbf{H}$ and the received vector is processed by the analog RF combiner at receiver, $\mathbf{W}_{rf}(t) \in \mathbb{C}^{N_r \times N_r^{rf}}$. The elements of the RF precoders and combiners have equal norm as they represent transmitter and receiver phase shifters. For the case of number of streams equal to the number of RF chains, the baseband matrices, $\mathbf{F}_{bb}(t) \in \mathbb{C}^{N_t^{rf} \times N_s}$ at transmitter and $\mathbf{W}_{bb}(t) \in \mathbb{C}^{N_r^{rf} \times N_s}$ at receiver, are identity matrices so we consider only RF/analog processing to formulate the channel estimation problem. The received signal after RF/analog processing, $\mathbf{y}_c(t) \in \mathbb{C}^{N_r \times 1}$ for $t = 1, \ldots, T$, is expressed as:

$$\mathbf{y}_c(t) = \mathbf{W}_{rf}^*(t)\mathbf{H}\mathbf{F}_{rf}(t)\mathbf{s}(t) + \mathbf{n}_c(t), \quad (4)$$

where $\mathbf{n}_c \in \mathbb{C}^{N_r \times 1}$ noise vector following the complex Gaussian distribution with i.i.d. entries, i.e., $\mathbf{n}_c \sim \mathcal{CN}(\mathbf{0}, \sigma^2 \mathbf{I}_{N_r})$. By concatenating all the T training sequences into the real-valued equivalent form we have:

$$\bar{\mathbf{y}} = \begin{bmatrix} \mathrm{Re}(\bar{\mathbf{y}}_c) \\ \mathrm{Im}(\bar{\mathbf{y}}_c) \end{bmatrix} = \bar{\mathbf{\Psi}} \begin{bmatrix} \mathrm{Re}(\mathbf{z}_c) \\ \mathrm{Im}(\mathbf{z}_c) \end{bmatrix} + \begin{bmatrix} \mathrm{Re}(\bar{\mathbf{n}}_c) \\ \mathrm{Im}(\bar{\mathbf{n}}_c) \end{bmatrix}, \quad (5)$$

where $\bar{\mathbf{\Psi}} = \begin{bmatrix} \mathrm{Re}(\bar{\mathbf{\Psi}}_c) & -\mathrm{Im}(\bar{\mathbf{\Psi}}_c) \\ \mathrm{Im}(\bar{\mathbf{\Psi}}_c) & \mathrm{Re}(\bar{\mathbf{\Psi}}_c) \end{bmatrix}^T \in \mathbb{R}^{2TN_r \times 2N_r N_t}$ and $\bar{\mathbf{y}}_\mathbf{c}, \bar{\mathbf{n}}_\mathbf{c}, \bar{\mathbf{\Psi}}_\mathbf{c}$ are the concatenated quantities for the received signal, the AWGN and the system matrix, respectively.

Let us denote the K-level quantization of $\bar{\mathbf{y}} \in \mathbb{R}^{2TN_r \times 1}$ as the function $\mathcal{Q}(.)$,

$$\bar{\mathbf{q}} = \mathcal{Q}(\bar{\mathbf{y}}), \quad (6)$$

where $\bar{\mathbf{q}} = [q_1 \ldots q_{2TN_r}]^T \in \mathbb{R}^{2TN_r \times 1}$. Each output element takes one of K distinct values with,

$$q_i^k = -l_i^k + \frac{\Delta}{2} + (k-1)\Delta, \forall k = 1, ..., K, \quad (7)$$

depending on the quantizer lower and upper thresholds $[l_i^k, u_i^k]$ where $l_i^k = -\kappa\sqrt{\mathbb{E}\{y_i^2\}}$ and $u_i^k = \kappa\sqrt{\mathbb{E}\{y_i\}}$, $\forall i$ and $\kappa \in [1, 5]$. The quantizer's step-size is given by $\Delta = \frac{u_i^k - l_i^k}{K}$, while the average power $\mathbb{E}\{y_i\}$ can be obtained via an automatic gain control (AGC) circuit.

III. Proposed Channel Estimation Solution

A. Problem Formulation

Following the beamspace representation of the sparse mmWave channel in (3), the system model of (4) can be rewritten into an equivalent form for the channel estimation problem, i.e.,

$$\mathbf{y}_c(t) = \underbrace{\left(\mathbf{s}^T(t)\mathbf{F}_{rf}^T(t)\hat{\mathbf{A}}_t \otimes \mathbf{W}_{rf}^*(t)\hat{\mathbf{A}}_r\right)}_{\mathbf{\Psi}_c(t)} \underbrace{\mathrm{vec}(\mathbf{Z})}_{\mathbf{z}} + \mathbf{n}_c(t), \quad (8)$$

ISBN 978-90-827970-1-5 © EURASIP 2018

thus, sparse estimation techniques can be utilized to recover the sparse vector $\mathbf{z}$.

Concerning the analog RF beamforming matrices, these are designed as random matrices [24] as we require sensing matrix to be random to be able to apply compressed sensing. The transmitter and the receiver share a pseudo-random key so receiver can predict the precoding matrix. In particular, the angles of precoding/combiner matrices are generated as random variables following a uniform distribution, i.e., $\tilde{\phi}_i(t) \sim \mathcal{U}(0, 2\pi)$. Then, for each training instance t and $\forall k = 1, \ldots, N_t, i = 1, \ldots, N_t^{rf}$ we use the matrix:

$$[\mathbf{F}_{rf}(t)]_{ki} = \frac{1}{\sqrt{N_t}} e^{j(k-1)\sin(\tilde{\phi}_i(t))}, \tag{9}$$

for precoding, and accordingly for the combiner at the receiver:

$$[\mathbf{W}_{rf}(t)]_{ki} = \frac{1}{\sqrt{N_t}} e^{j(k-1)\sin(\tilde{\phi}_i(t))}. \tag{10}$$

To overcome the quantization non-linearity effects at the receiver, we employ quantization dithering [25]. In this work we consider a simple type of dithering termed as non-subtractive random dithering. Specifically, we assume that a Gaussian random signal with zero mean, i.e., $\bar{\mathbf{d}} \sim \mathcal{N}(\mathbf{0}, \sigma_d^2 \mathbf{I})$ is added to the input, thus, the overall system is described as:

$$\bar{\mathbf{r}} = \mathcal{Q}\big(\bar{\mathbf{\Psi}}\mathbf{z} + \bar{\mathbf{n}} + \bar{\mathbf{d}}\big) \in \mathbb{R}^{2TN_r \times 1}, \tag{11}$$

where $\bar{\mathbf{d}} \in \mathbb{R}^{2TN_r \times 1}$ is the control signal. The overall noise can be modelled as $\bar{\mathbf{n}} + \bar{\mathbf{d}} \sim \mathcal{N}\big(\mathbf{0}, \sigma^2 \mathbf{I}\big)$, where $\sigma^2 = \sigma_n^2 + \sigma_d^2$.

B. EM-SURE-GAMP Solution for Channel Estimation

To solve the non-linear sparse channel estimation problem of (8) we obtain an approximation of the maximum a-posteriori channel estimator via the EM algorithm [11], for l-th iteration, i.e.,

$$\mathbb{E}_{\bar{\mathbf{y}}|\bar{\mathbf{r}},\mathbf{z}} \left\{ \frac{\partial}{\partial \mathbf{z}} \ln p(\bar{\mathbf{r}}, \bar{\mathbf{y}}|\mathbf{z}^l) \right\} = 0, \tag{12}$$

where the conditional probability density function (PDF) involving $\bar{\mathbf{r}}$ and $\bar{\mathbf{y}}$ random variables is given by [26] as follows:

$$p(\bar{\mathbf{r}}, \bar{\mathbf{y}}|\mathbf{z}) = \mathbb{I}_{D(\bar{\mathbf{r}})}(\bar{\mathbf{y}}) \frac{1}{(2\pi\sigma^2)^{2TN_r \times 1/2}} e^{\frac{-\|\bar{\mathbf{y}} - \bar{\mathbf{\Psi}}\mathbf{z}\|_2^2}{2\sigma^2}}. \tag{13}$$

The EM algorithm is defined by the following two steps for the $(l+1)$-th iteration:

- **E-step:** Compute $\mathbf{b}^l = [b_1^l, \ldots, b_{2TN_r}^l]$ with

$$b_i^l = -\frac{\sigma}{\sqrt{2\pi}} \frac{e^{-\frac{(l_i - [\bar{\mathbf{\Psi}}\mathbf{z}^l]_i)^2}{2\sigma^2}} - e^{-\frac{(u_i - [\bar{\mathbf{\Psi}}\mathbf{z}^l]_i)^2}{2\sigma^2}}}{\mathrm{erf}(\frac{-l_i + [\bar{\mathbf{\Psi}}\mathbf{z}^l]_i}{\sqrt{2}\sigma}) - \mathrm{erf}(\frac{-u_i + [\bar{\mathbf{\Psi}}\mathbf{z}^l]_i}{\sqrt{2}\sigma})}, \tag{14}$$

  where l_i, u_i are the lower and upper bounds for the i^{th} quantized sample of the quantizer for $[\bar{\mathbf{\Psi}}\mathbf{z}^l]_i$ respectively; $\mathrm{erf}(\cdot)$ is the error function.

- **M-step:** Estimate the sparse channel $\mathbf{z}^{l+1} \in \mathbb{R}^{2N_r N_t \times 1}$ via solution of the linear system of equations:

$$\mathbf{A}\mathbf{z}^{l+1} = \boldsymbol{\delta}_l, \tag{15}$$

with $\boldsymbol{\delta}_l \triangleq \bar{\mathbf{\Psi}}^T \bar{\mathbf{\Psi}} \mathbf{z}^l + \mathbf{b}^l$ and $\mathbf{A} \triangleq \bar{\mathbf{\Psi}}^T \bar{\mathbf{\Psi}} + \mathbf{C}_h^{-1}$, where $\mathbf{C}_h^{-1}$ is the correlation matrix based on the channel known statistics.

Algorithm 1: EM-SURE-GAMP algorithm

1 **Initialization**: $\hat{\mathbf{z}}^1 = \mathbf{0}, \boldsymbol{\xi}^0 = \mathbf{0}, c^1 = \frac{1}{2N_r N_t}, \tau_z^1 = 1.$
2 **for** t = $1, \ldots, T_{max}$ **do**
3 $\quad \boldsymbol{\gamma}^t = \mathbf{A}\hat{\mathbf{z}}^t$
4 $\quad \tau_p^t = \frac{1}{2N_r N_t} \|\mathbf{A}\|_F^2 \tau_z^t$
5 $\quad \mathbf{p}^t = \boldsymbol{\gamma}^t - \tau_p^t \boldsymbol{\xi}^{t-1}$
6 $\quad$ Update $\boldsymbol{\delta}_l$ using EM-steps as indicated in (15)
7 $\quad \boldsymbol{\xi}^t = \mathbb{E}_{p(\boldsymbol{\gamma}^t|\mathbf{p}^t, \tau_p^t, \boldsymbol{\delta}_l)}[\boldsymbol{\gamma}^t|\mathbf{p}^t, \tau_p^t, \boldsymbol{\delta}_l]$
8 $\quad \tau_\xi^t = \frac{1}{2N_r N_t \tau_p^t} \left[1 - \frac{\mathrm{Var}_{p(\boldsymbol{\gamma}^t|\mathbf{p}^t, \tau_p^t, \boldsymbol{\delta}_l)}[\boldsymbol{\gamma}^t|\mathbf{p}^t, \tau_p^t, \boldsymbol{\delta}_l]}{\tau_p^t}\right]$
9 $\quad \frac{1}{\tau_\beta^t} = \frac{1}{2N_r N_t} \|\mathbf{A}\|_F^2 \tau_\xi^t$
10 $\quad \boldsymbol{\beta}^t = \hat{\mathbf{z}}^t + \tau_\beta^t \mathbf{A}^* \boldsymbol{\xi}^t$
11 $\quad \boldsymbol{\theta}^t = H_t(\boldsymbol{\beta}^t, c^t)$
12 $\quad \hat{\mathbf{z}}^{t+1} = f_t(\boldsymbol{\beta}^t, c^t|\boldsymbol{\theta}^t)$
13 $\quad \tau_z^{t+1} = \tau_\beta^t f_t'(\boldsymbol{\beta}^t, c^t|\boldsymbol{\theta}^t)$
14 $\quad c^{t+1} = \frac{1}{2N_r N_t} ||\tau_\beta^t \boldsymbol{\xi}^t||_2^2$
15 **end for**

The linear channel estimation problem in (15) can be considered similar to the noisy quantized CS problem [27]; among the numerous existing algorithms for sparse inverse linear problems, AMP-based solver has been shown to converge faster, i.e. in few iterations, with predictable dynamics together with low computational complexity. In its original formulation for l_1-minimization [28], AMP is a designed as a variant of a soft-thresholding iterative algorithm; in [29], [30] extensions of AMP have been used to handle wide class of random sensing matrices and for sparse learning applications. Generally AMP family of algorithms has been proven to converge for the class of right orthogonal random matrices; to reduce the convergence problems with general structured random matrices, damping is often used. However, for our system model we do not need to perform damping on the update of the messages.

In particular, AMP-based algorithms perform a sequence of MMSE estimations of the estimated measurement vector $\boldsymbol{\gamma}^t = \bar{\mathbf{\Psi}}\hat{\mathbf{z}}^t$, such as in line 3 of Algorithm 1, where $\hat{\mathbf{z}}^t$ refers to the estimate of the vector $\mathbf{z}^{l+1}$ for the M-step in (15) and l is the EM iteration index. Regarding the MMSE estimator for $\boldsymbol{\gamma}^t$, since the channel noise model in (11) is quantized Gaussian as it is modeled as the quantization function, we need to adopt the generalized version of AMP (GAMP) [31] whose computation is detailed in the Algorithm 1 where the expectation is over the posterior probability $p(\boldsymbol{\gamma}^t|\mathbf{p}^t, \tau_p^t, \boldsymbol{\delta}_l)$ which is dependent on the quantizer function $\mathcal{Q}$ through (14). $\boldsymbol{\delta}_l$ represents the vector of measurements updated using the EM-steps as indicated in (15). In line 8 of Algorithm 1, $\mathrm{Var}_{p(\boldsymbol{\gamma}^t|\mathbf{p}^t, \tau_p^t, \boldsymbol{\delta}_l)}[\cdot]$ represents the Variance of the conditional probability distribution $p(\boldsymbol{\gamma}^t|\mathbf{p}^t, \tau_p^t, \boldsymbol{\delta}_l)$. Regarding the MMSE estimator for $\hat{\mathbf{z}}^t$, standard AMP [28] is based on the assumption that the prior $p(\hat{\mathbf{z}}^t)$ is precisely defined and, therefore, it is possible to derive the associated MMSE estimator.

In this work, we utilize a variant, named SURE-GAMP,

ISBN 978-90-827970-1-5 © EURASIP 2018

which derives specific MMSE estimators tailored for the dithered system model in (11) as follows. The SURE approach [19] aims to find the denoiser within a class with the least MSE by optimizing the free parameters $\boldsymbol{\theta}^t$ of some piecewise kernel functions $f_t(\cdot|\boldsymbol{\theta}^t)$ in order to obtain an optimal adaptive non linearity; moreover, the optimization of the denoiser does not require knowledge of the prior distribution. In the simulations, SURE-GAMP uses a family of parameterized denoising functions for the class of Bernoulli Gaussian signals, which can be analyzed through Gaussian-mixture distribution as well [18]. At each iteration, the parametric SURE-GAMP algorithm adaptively chooses the best denoiser, i.e. the one with the least MSE, by selecting the parameters $\boldsymbol{\theta}^t$ which correspond to the minimum of the selection function H_t, such as in line 11 of Algorithm 1, dependent on the noisy data $\boldsymbol{\beta}^t$ and the estimate of the effective noise variance c^t which leads to solving the following optimization problem:

$$\begin{aligned} \boldsymbol{\theta}^t &= H_t(\boldsymbol{\beta}^t, c^t) \\ &= \arg\min_{\boldsymbol{\theta}} \mathbb{E}[f(\boldsymbol{\beta}^t, c^t|\boldsymbol{\theta}) - \boldsymbol{\beta}^t)^2 + 2c^t f'(\boldsymbol{\beta}^t, c^t|\boldsymbol{\theta})] \end{aligned} \tag{16}$$

In [19], authors have shown that this optimization is equivalent to solving a linear system of equations whose dimension equals the number of kernel functions which are the number n_{ker} of basis functions representing $f(\cdot|\boldsymbol{\theta})$ ($n_{ker} = 3$, in the simulations). Therefore, the overall complexity of SURE-GAMP is dominated by the matrix-vector multiplications in lines 3 and 10 of Algorithm 1, whose order is $\mathcal{O}((N_r N_t)^2)$. The EM steps as shown in (14) and (15) are combined with the SURE-GAMP algorithm to avoid the need of specifying a prior probability on $\mathbf{z}^{l+1}$. The algorithm converges after a few iterations when the solution close to minimum MSE is achieved.

IV. Simulation Results

This section shows the performance results obtained for the proposed EM-SURE-GAMP algorithm and the comparison is made with the EM-GAMP solution. Reference [31] suggests the computation of the minimum MSE of the estimate; combined with EM steps we can plot the MSE results of EM-GAMP algorithm to compare with the proposed solution. Following the condition $N_t^{rf} \leq N_t$ and $N_r^{rf} \leq N_r$ for a hybrid analog-digital MIMO architecture, we consider a simple case of $N_t = 8$, $N_r = 8$, and the number of RF chains and streams equal to the number of antennas, i.e., $N_t^{rf} = N_r^{rf} = N_s = 8$. It provides us easier computation for the analog precoder and combiner matrices. We can also consider fewer RF chains and streams than the number of antennas [32] to observe the channel estimation performance plots. The number of multipaths is 5 and due to low overload probability, the value of κ used in the quantization (see Section II) is 4. We run the proposed algorithm for $T_{max} = 1$ and 100 EM iterations. The performance results are obtained for 100 Monte-Carlo realizations each.

Fig. 2 shows the mean square error (MSE) variations with respect to (w.r.t.) the SNR when comparing the proposed EM-SURE-GAMP algorithm with EM-GAMP for 1-bit, 2-bits, and 3-bits resolution ADCs. We can observe that the proposed algorithm achieves better MSE performance for both low and high SNR regimes. For example at an SNR of 10 dB, the SURE algorithm variant outperforms EM-GAMP by about 3 dB in MSE terms for 1-bit quantization. For 2- and 3-bits, the MSE gain is around 2 dB.

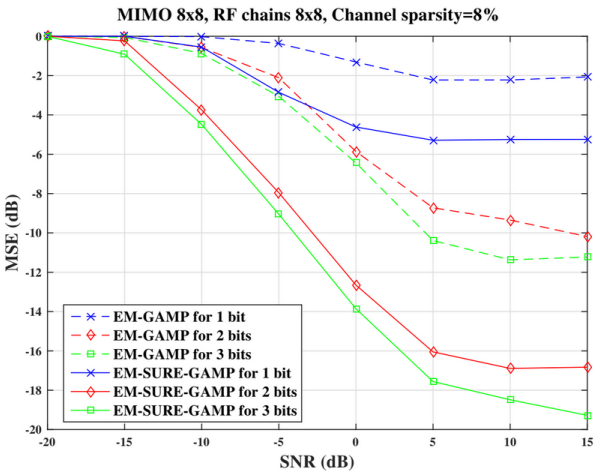

Fig. 2: MSE versus SNR.

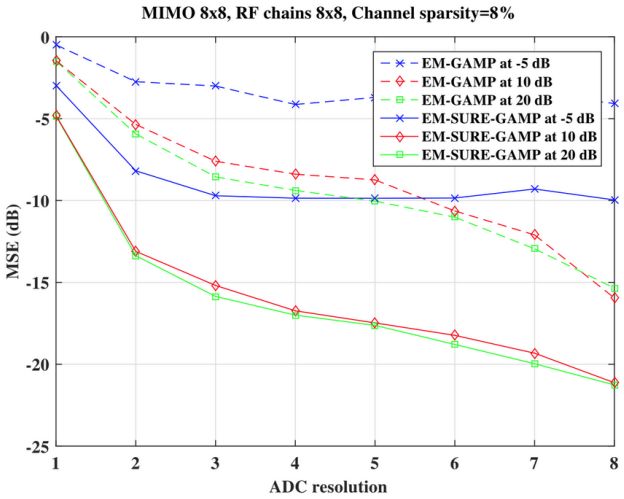

Fig. 3: MSE versus the number of ADC bits.

Fig. 3 again shows that EM-SURE-GAMP performs better than EM-GAMP when MSE is plotted against the number of quantization bits for different values of SNR such as -5 dB, 10 dB, and 20 dB. The training length for Fig. 2 and Fig. 3 is $T = 2^{11}$, and EM-SURE-GAMP exhibits good performance for a channel sparsity level, i.e., ratio of non-zero entries of the beamspace channel and $N_r \times N_t$, of 8%. It can be seen for example that with 3 bits resolution, a significant gain in MSE for the SURE variant of around 6-7 dB compared to EM-GAMP is observed for all SNR values.

Fig. 4 exhibits that the EM-SURE-GAMP solution outperforms EM-GAMP solution w.r.t. the training length for a range of training sequence lengths of 64 to 2048 and converges more quickly than EM-GAMP for a channel sparsity level of 8%, 15 dB SNR, when 1-bit, 2-bits, and 3-bits ADC resolutions are considered.

ISBN 978-90-827970-1-5 © EURASIP 2018

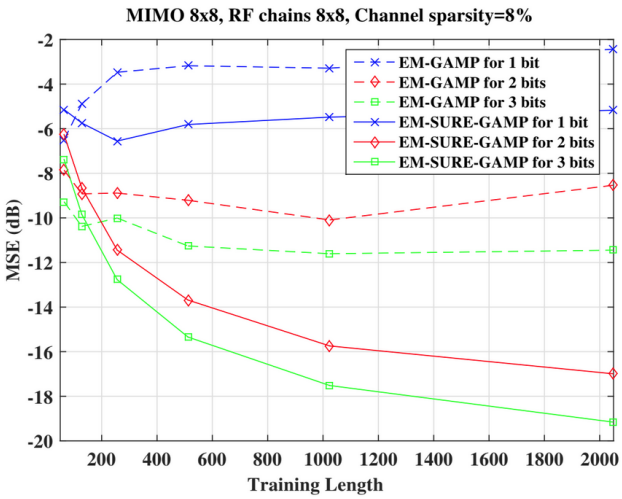

Fig. 4: MSE versus the training length T.

V. Conclusion

This paper proposes an efficient algorithm based on the approximate message passing (AMP) framework to estimate the channel in a mmWave MIMO system with a hybrid analog-digital architecture and low-resolution ADCs at the receiver. EM-SURE-GAMP is exploited to estimate the channel which provides the flexibility to avoid strong assumptions on the channel priors where SURE, depending on the noisy observation, is minimized to adaptively optimize the denoiser within the parametric class at each iteration. When compared with the expectation-maximization generalized AMP (EM-GAMP) solution, the mean square error (MSE) performs better with respect to low and high SNR regimes, the number of ADC bits, and the training length.

References

[1] R. W. Heath et al., "An overview of signal processing techniques for millimeter wave MIMO systems", *IEEE Journ. Sel. Topics Signal Process.*, vol. 10, no. 3, pp. 436-453, Apr. 2016.

[2] B. Le et al., "Analog-to-digital converters", *IEEE Signal Process. Mag.*, vol. 22, no. 6, pp. 69-77, Nov. 2005.

[3] R. Walden, "Analog-to-digital converter survey and analysis", *IEEE Journ. Sel. Areas Commun.*, vol. 17, no. 4, pp. 539-550, Apr. 1999.

[4] J. Choi et al., "Near maximum-likelihood detector and channel estimator for uplink multiuser massive MIMO systems with one-bit ADCs", *IEEE Trans. Commun.*, vol. 64, no. 5, pp. 2005-2018, May. 2016.

[5] S. Jacobsson et al., "One-bit massive MIMO: channel estimation and high-order modulations", *IEEE Int. Conf. Commun. Workshop*, pp. 1304-1309, June 2015.

[6] A. Alkhateeb et al., "Channel estimation and hybrid precoding for millimeter wave cellular systems", *IEEE Journ. Sel. Topics Signal Process.*, vol. 8, no. 5, pp. 831-846, Oct. 2014.

[7] J. Lee et al., "Exploiting spatial sparsity for estimating channels of hybrid MIMO systems in millimeter wave communications", *IEEE Global Commun. Conf.*, pp. 3326-3331, Dec. 2014.

[8] P. Schniter, and A. Sayeed, "Channel estimation and precoder design for millimeter-wave communications: the sparse way", *IEEE Asilomar Conf. Sig. Sys. Comp.*, pp. 273-277, Nov. 2014.

[9] J. Mo et al., "Capacity analysis of one-bit quantized MIMO systems with transmitter channel state information", *IEEE Trans. Signal Process.*, vol. 63, no. 20, pp. 5498-5512, Oct. 2015.

[10] C. Rusu et al., "Low resolution adaptive compressed sensing for mmWave MIMO receivers", *IEEE Asilomar Conf. Sig. Sys. Comp.*, pp. 1138-1143, Nov. 2015.

[11] J. Mo et al., "Channel estimation in millimeter wave MIMO systems with one-bit quantization", *IEEE Asilomar Conf. Sig. Sys. Comp.*, pp. 957-961, Nov. 2014.

[12] O. Orhan et al., "Low power analog-to-digital conversion in millimeter wave systems: Impact of resolution and bandwidth on performance", *2015 Info. Theory Appl. Workshop, San Diego, CA*, pp. 191-198, 2015.

[13] L. Fan et al., "Uplink achievable rate for massive MIMO systems with low-resolution ADC", *IEEE Commun. Letters*, vol. 19, no. 12, pp. 2186-2189, Oct. 2015.

[14] M. T. Ivrlac, and J. A. Nossek, "On MIMO channel estimation with single-bit signal-quantization", in *Proc. IEEE Smart Antenn. Workshop*, Feb. 2007.

[15] A. Mezghani et al., "Multiple parameter estimation with quantized channel output", in *Proc. Int. ITG Workshop Smart Antenn.*, pp. 143-150, Oct. 2010.

[16] J. Vila, and P. Schniter, "Expectation-maximization Gaussian-mixture approximate message passing", *IEEE Trans. Signal Process.*, pp. 4658-4672, May 2014.

[17] S. Rangan et al., "Vector approximate message passing", *arXiv:1610.03082*, Oct. 2016.

[18] J. Mo et al., "Channel estimation in broadband millimeter wave MIMO systems with few-bit ADCs", in *IEEE Trans. Signal Process.*, vol. 66, no. 5, pp. 1141-1154, March 2018.

[19] C. Guo, and M. E. Davies, "Near optimal compressed sensing without priors: parametric SURE approximate message passing", *IEEE Trans. Signal Process.*, vol. 63, no. 8, Apr. 2015.

[20] S. Singh et al., "Interference analysis for highly directional 60-GHz mesh networks: The case for rethinking medium access control", *IEEE/ACM Trans. Netw.*, vol. 19, no. 5, pp. 1513-1527, Oct. 2011.

[21] C. Balanis, *Antenna Theory*, Wiley, 1997.

[22] J. Brady et al., "Beamspace MIMO for millimeter-wave communications: System architecture, modeling, analysis, and measurements", *IEEE Trans. Antenn. Propag.*, vol. 61, no. 7, pp. 38143827, Jul. 2013.

[23] L. Dai et al., "Beamspace channel estimation for millimeter-wave massive MIMO systems with lens antenna array", in *2016 IEEE/CIC Int. Conf. Commun. China (ICCC)*, pp. 16, July 2016.

[24] D. L. Donoho, "Compressed sensing", *IEEE Trans. Info. Theory*, vol. 52, no. 4, pp. 12891306, Apr. 2006.

[25] R. A. Wannamaker, *The theory of dithered quantization*, National Library Canada, 1997.

[26] O. Dabeer and E. Masry, "Multivariate signal parameter estimation under dependent noise From 1-bit dithered quantized data", *IEEE Trans. Info. Theory*, vol. 54, no. 4, pp. 1637-1654, April 2008.

[27] U. S. Kamilov et al., "Message-passing de-quantization with applications to compressed sensing", *IEEE Trans. Signal Process.*, vol. 60, no. 12, pp. 6270-6281, 2012.

[28] D. Donoho et al., "Message-passing algorithms for compressed sensing", *Proc. Nat. Acad. Sci.*, vol. 106, no. 45, pp.18 914-18 919, 2009.

[29] M. Al-Shoukairi et al., "A GAMP-based low complexity sparse bayesian learning algorithm", *IEEE Trans. Signal Process.*, vol. 66, no. 2, pp. 294-308, Jan. 2018.

[30] J. Ma and L. Ping, "Orthogonal AMP", *IEEE Access*, vol. 5, pp. 2020-2033, 2017.

[31] S. Rangan, "Generalized approximate message passing for estimation with random linear mixing", *IEEE Int. Symp. Info. Theory Proc.*, pp. 2168-2172, 2011.

[32] A. Kaushik et al., "Sparse hybrid precoding and combining in millimeter wave MIMO systems", *Radio Propag. Tech. 5G, Durham, UK*, pp. 1-7, Oct. 2016.

ISBN 978-90-827970-1-5 © EURASIP 2018